



# Study on preparation and performances of cellulose acetate forward osmosis membrane

Min Shang<sup>1</sup> · Baoli Shi<sup>1</sup>

Received: 8 January 2018 / Accepted: 6 July 2018 / Published online: 9 July 2018  
© Institute of Chemistry, Slovak Academy of Sciences 2018

## Abstract

Cellulose acetate (CA) forward osmosis (FO) membranes were prepared via a phase inversion process. CA was used as membrane material for FO. Acetone and 1,4-dioxane were employed as solvent. Polyvinylpyrrolidone (PVP), maleic acid, and methanol were applied as additives. An orthogonal experiment was performed to optimize the ratio of every component in the casting solution. The membrane with best performance was selected to concentrate an anthocyanin solution. Saturated sucrose solution (about 60°Brix) was fit for using as draw solution in the concentration experiment. Water flux, porosity, and rejection rate were measured to evaluate the membrane properties. Reverse water rinsing was used in cleaning membrane that was fouled by anthocyanin solution. Results showed that under membrane thickness of 100  $\mu\text{m}$ , coagulation temperature at room temperature, and evaporation time of 30 s, the optimum components in casting solution were 13% CA, 45% 1,4-dioxane, 31% acetone, 2% maleic acid, 3% PVP, and 6% methanol. In the concentration experiment, the prepared FO membrane showed water flux of 2.04  $\text{L m}^{-2} \text{h}^{-1}$  and rejection rate of 98.61%. In the membrane cleaning experiment, the water flux of the FO membrane recovered 87.51% after rinsing for 1 h. The prepared membranes and previously published membranes were compared which showed the prepared membrane could significantly improve the rejection rate for anthocyanin solution.

**Keywords** Cellulose acetate · Forward osmosis membrane · Anthocyanin

## Introduction

Forward osmosis (FO) is a membrane technology driven by osmotic pressure operated at zero or low pressure (Lee et al. 2010; Xu et al. 2017). In this process, a selective semi-osmotic membrane is used, and water flows from the side with higher chemical potential to the lower side (Gao et al. 2018; Gray et al. 2006; Qasim et al. 2017). FO can achieve the separation of water in the solution at the molecular level (Ge et al. 2013). Compared with the pressure-driven membrane in reverse osmosis, the FO membrane has higher water flux, lower tendency for membrane fouling, and higher energy efficiency (Chung et al. 2012; Cath et al. 2006; Phuntsho et al. 2013). Thus, FO can be applied to desalination (Roy et al. 2016; Akther et al. 2015), wastewater recovery (Lutchmiah et al. 2014), food processing (Law and Mohammad 2017), and other fields.

Anthocyanin is a natural pigment with many important nutritional and pharmacological functions, such as for maintaining the skin, enhancing eyesight, and delaying the aging of brain nerves (Baron et al. 2017). The concentration of anthocyanin solution is an important parameter in the production of anthocyanin products. Nowadays, heat treatment and freeze concentration are usually applied during production (Jafari et al. 2017). However, these methods do not only influence the nutritional value and taste of the anthocyanin products, but they also entail high production costs (Nayak and Rastogi 2010). For food processing, FO has the advantage of concentrating the feed solution without the need for high pressure or high temperature of this solution (Jiao et al. 2004; Petrotos and Lazarides 2001). In a related study, the use of FO membrane to process fruit juice has stimulated our attention (Babu et al. 2006; Chanukya and Rastogi 2017). However, commercial FO membrane hardly achieves complete rejection of anthocyanin solution.

Cellulose acetate (CA) has several advantages such as high selectivity, good hydrophilicity, safety, and low cost (Etemadi et al. 2017; Waheed et al. 2014). This material is ideal for preparing FO membranes. Sucrose is cheaper

✉ Baoli Shi  
shi\_baoli\_nefu@163.com

<sup>1</sup> College of Science, Northeast Forestry University, Harbin 150040, Heilongjiang, China

than other sugar in China. Because the solubility of sucrose in water is large, a high osmotic pressure will be produced if it is used as draw agent. Selection of additive species in the casting solution is quite important when preparing CA membrane to enhance the application of the FO membrane in rejecting anthocyanin molecules. Sairam et al. prepared an FO membrane by adding maleic acid as additive (Sairam et al. 2011). The resultant membrane showed remarkably higher water flux and rejection rate than those of HTI commercial FO membrane. Malek et al. used PVP as additive to prepare an FO membrane and obtained a membrane with improved hydrophilicity and permeability (Malek et al. 2017). Chen et al. proposed the preparation of an FO membrane using mixed additives (Chen et al. 2017). The results showed membranes with enhanced structures and properties. In this study, PVP, maleic acid, and methanol were used as additives to improve the permeability of an FO membrane. Acetone and 1,4-dioxane were selected as solvents. Orthogonal experiment was performed to determine the best ratio of every component in the casting solution. The membrane with best performance of all components was used to concentrate an anthocyanin solution. Reverse water rinsing was used in cleaning membrane that was fouled by anthocyanin solution.

## Experimental

### Materials

CA with approximately 54.5–56.0% acetic acid bonded was purchased from Sinopharm Chemical Reagent Co., Ltd, China. Analytical grade 1,4-dioxane and acetone were used as solvent which were purchased from Tianjin Fuyu Fine Chemicals Co., Ltd, China. Analytical grade polyvinylpyrrolidone (PVP-K30), maleic acid and methanol were purchased from Shanghai Blue Season Technology Development Co., Ltd, Tianjin Guangfu Fine Chemical Research Institute, and Tianjin Tianli Chemical Reagent Co., Ltd, China. Analytical grade *n*-butanol was purchased from Tianjin Fuyu Fine Chemicals Co., Ltd, China. Food-grade sucrose was purchased from Nanjing juice sugar industry Co., Ltd, China. Deionized water was used both in the membrane preparation process and in the membrane performance test experiment. *Lonicera edulis* anthocyanins (main component cyanidin-3-*O*-glucoside) were made in our laboratory.

### Membrane preparation

A certain amount of PVP was added to a dry conical flask and dissolved in methanol. Then, 5 g of dried CA and solvents (1,4-dioxane and acetone) were added to the flask. Finally, maleic acid was dissolved in the mixed solvent.

After a few hours of standing at room temperature, the casting solution was mixed by a glass bar. The mixed solution was allowed to settle until it bubbled completely. A nonwoven fabric was fixed on a clean glass plate. The casting solution was poured on one end of the nonwoven fabric and cast using a 100- $\mu\text{m}$  casting knife. After standing in air for a few seconds, the nonwoven fabric was moved into a water bath. The fabricated membrane was stored in deionized water prior to use. The ratio of each component in the casting solution was varied.

### Variation in ratio of components in casting solution

The ratio of each component in the casting solution will affect membrane structure and consequently influence remarkably the membrane performance. Five factors were designed, and four different levels were formulated for each factor. The parameters of the orthogonal experimental design are listed in Table 1. 16 kinds of different membranes were prepared. Each membrane was cut into three small pieces with the same area. The three small pieces membranes were tested for 3 h, respectively. The FO membranes were prepared under the following conditions: membrane thickness, 100  $\mu\text{m}$ ; coagulation temperature, room temperature; and evaporation time, 30 s.

### Measurement of flux and rejection

The prepared FO membrane was cut into the appropriate size and installed in a homemade test cell with an effective area of  $1.35 \times 10^{-3} \text{ m}^2$ . Figure 1 shows the schematic diagram of the FO experiment. A sufficient amount of  $0.27 \text{ g L}^{-1}$  anthocyanin solution as feed solution and sucrose solution as draw solution were placed in membrane two sides with mode II (mode I: feed solution towards the support layer, mode II: feed solution towards active layer). The beakers containing the solutions were sealed with cling-film to prevent the evaporation of water. The solutions were circulated by peristaltic pumps for 3 h. Changes in the mass of the draw solution in the beaker were monitored by an electronic

**Table 1** Factors and levels of the orthogonal experiment

Level	Factor				
	A (%)	B (%)	C (%)	D (%)	E (%)
1	13	27	1	1	5
2	14	36	2	2	6
3	15	45	3	3	7
4	16	54	4	4	8

A: mass concentration of CA. B: mass concentration of 1,4-dioxane. C: mass concentration of maleic acid. D: mass concentration of PVP. E: mass concentration of methanol

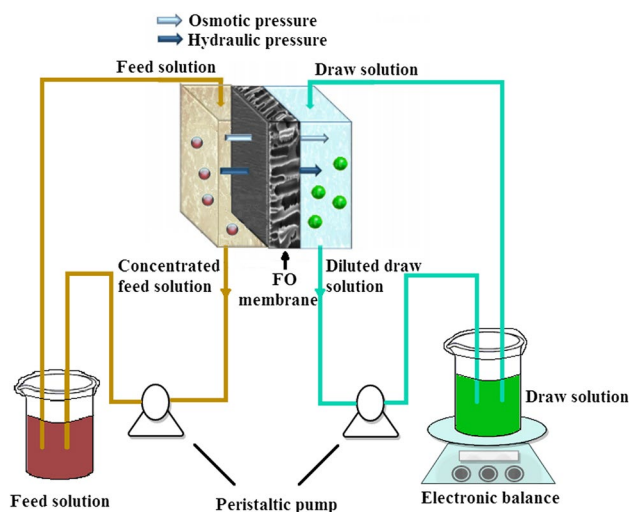


Fig. 1 Schematic diagram of the FO experiment

balance. To research the influence of concentration of draw solution on flux, four sucrose solutions with the concentration of 30, 40, 50 and 60°Brix (saturated solution) were used as the draw solutions.

Water flux ( $J_w$ ,  $L\ m^{-2}\ h^{-1}$ ) was measured and calculated as follows:

$$J_w = \frac{\Delta W}{\rho \times S_{\text{eff}} \times t}, \quad (1)$$

where  $\Delta W$  (kg) is the change in the mass of water permeated from the feed solution to the draw solution,  $t$  (h) is the circulation time,  $S_{\text{eff}}$  ( $m^2$ ) is the effective membrane area, and  $\rho$  ( $kg\ m^{-3}$ ) is the water density.

The rejection rate ( $R$ , %) was calculated as follows:

$$R = \left[ 1 - \frac{C_1}{C_0} \right] \times 100\%, \quad (2)$$

where  $C_0$  is the concentration of anthocyanin solution before circulation and  $C_1$  is the permeate concentration of anthocyanin solution after 3 h of circulation. The permeate concentration was measured by a homemade illuminometer device which was composed mainly of a digital illuminometer (TES-1332A) and a light source. The resolution of the homemade illuminometer device was 0.001 g/L.

### Measurement of membrane porosity

The average porosity ( $P$ , %) of the membranes was measured by the weight method (Asghar et al. 2018; Babu and Murthy 2017; Boriboon et al. 2018; Cui et al. 2017; Li et al.

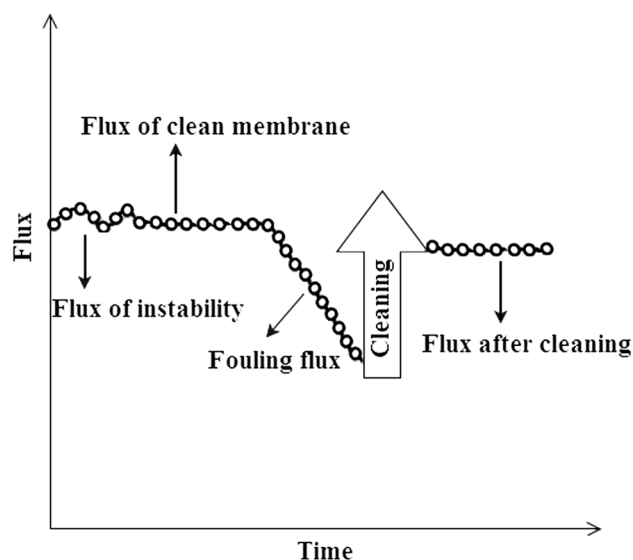


Fig. 2 Membrane fouling and cleaning protocol

2009; Rabiee et al. 2015). The porosity was calculated by the following equation:

$$P = \frac{W_2 - W_1 - W_3}{\rho' \times S \times l}, \quad (3)$$

where  $W_1$  and  $W_2$  are the initial mass of the dry membranes, the mass after immersing in *n*-butanol for 12 h, respectively;  $W_3$  is the mass of the nonwoven fabric after immersing in *n*-butanol for 12 h;  $\rho'$  is the density of *n*-butanol,  $S$  ( $m^2$ ) is the area of the membranes and  $l$  ( $\mu m$ ) is the thickness of the membranes.

### Membrane fouling and cleaning

Figure 2 illustrates the protocol for the fouling and cleaning experiments. First, the FO membrane was stabilized for at least 30 min with deionized water as the feed solution and saturated sucrose solution as the draw solution, until a stable water flux was achieved. And then the pure water flux was recorded before fouling tests. Next anthocyanin solution was used as the feed solution and saturated sucrose solution was used as the draw solution. After the fouling experiments, the feed solution and draw solutions were changed into saturated sucrose solution and deionized water, respectively. FO membrane was rinsed in reverse for 1, 3, 5 h. The water flux was measured again after cleaning.

**Table 2** Results of orthogonal experiment

Number	A	B	C	D	E	Flux ( $L\ m^{-2}\ h^{-1}$ )	Porosity (%)	Rejection rate (%)
1	1	1	1	1	1	0.85	44.15	97.32
2	1	2	2	2	2	1.75	66.65	98.10
3	1	3	3	3	3	1.65	64.76	97.63
4	1	4	4	4	4	1.09	48.99	98.35
5	2	1	2	3	4	1.38	39.91	97.89
6	2	2	1	4	3	0.97	40.14	98.67
7	2	3	4	1	2	1.53	52.87	98.37
8	2	4	3	2	1	1.13	40.95	98.31
9	3	1	3	4	2	0.89	40.06	98.59
10	3	2	1	3	1	1.56	37.14	98.39
11	3	3	4	2	4	0.84	51.26	98.90
12	3	4	2	1	3	1.40	44.93	98.74
13	4	1	4	2	3	0.83	27.67	98.95
14	4	2	3	1	4	0.70	35.49	99.39
15	4	3	2	4	1	1.23	54.27	98.62
16	4	4	1	3	2	1.28	52.36	98.73

**Table 3** Average flux results

Project	A	B	C	D	E
$\bar{K}_1$	1.34	0.99	1.17	1.12	1.19
$\bar{K}_2$	1.25	1.25	1.44	1.14	1.36
$\bar{K}_3$	1.17	1.31	1.09	1.47	1.21
$\bar{K}_4$	1.01	1.23	1.07	1.05	1.00

$\bar{K}_n$  is average flux result at each level for each factor

**Table 4** Average porosity results

Project	A	B	C	D	E
$\bar{k}_1$	56.14	37.95	43.45	44.36	44.13
$\bar{k}_2$	43.47	44.86	51.44	46.63	52.98
$\bar{k}_3$	43.35	55.79	45.32	48.54	44.38
$\bar{k}_4$	42.45	46.81	45.20	45.87	43.91

$\bar{k}_n$  is average porosity at each level for each factor

## Membrane characterization

The surface of the fractured membrane was coated with gold, and the surface morphology was observed by a scanning electron microscope (SEM) (FEI Quan Ta200 SEM, Holland). The contact angle of water at the surface of the membrane was measured by a contact angle measuring instrument (JC2000A) at room temperature. 5  $\mu$ L of distilled water was dripped on the membranes to test. Measurements were taken five times for one membrane and the average value was obtained. The chemical composition of the membrane surface was analyzed by attenuated total reflectance-Fourier transform infrared (ATR-FTIR) spectroscopy (Nicolet IS10). The measurement range was 4000–500  $cm^{-1}$  with a resolution of 4  $cm^{-1}$ .

## Results and discussion

### Orthogonal experimental results

The results of the orthogonal experiments are listed in Table 2. The five factors influenced water flux, rejection rate, and porosity under a single factor. The rejection rates were all over 97%.

### Optimum ratio of component in the casting solution

The average flux and porosity of the five factors of the casting solution are listed in Tables 3 and 4, respectively. Figure 3 shows the variations in the flux and porosity of each factor, and the tendencies were basically the same. The best combinations of casting solution conditions are identical, that is,  $a_1b_3c_2d_3e_2$ . Thus, the ratios of the components in the casting solution were 13% CA, 45% 1,4-dioxane, 2% maleic acid, 3% PVP, 31% acetone, and 6% methanol.

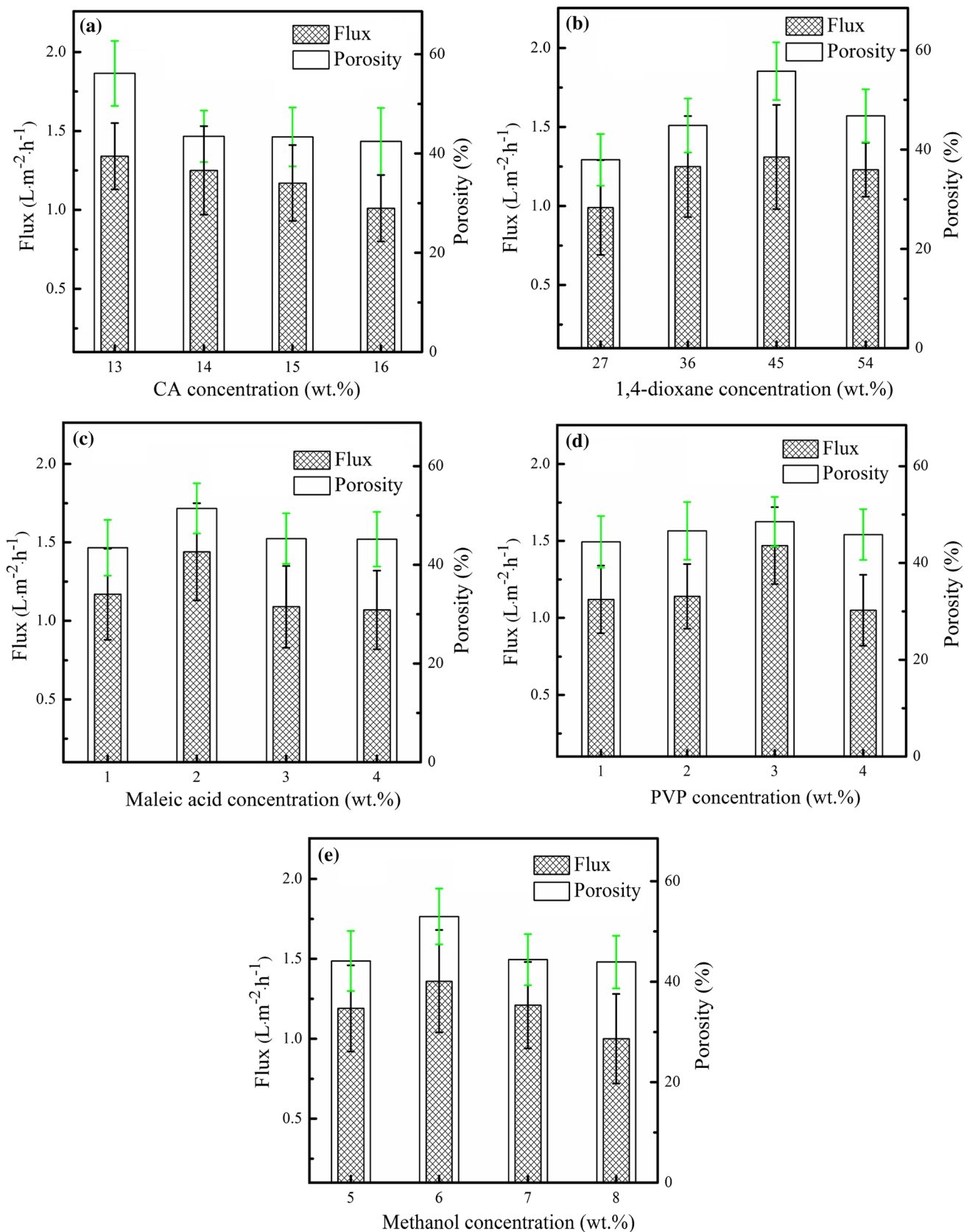


Fig. 3 Variation in the flux and porosity for each factor

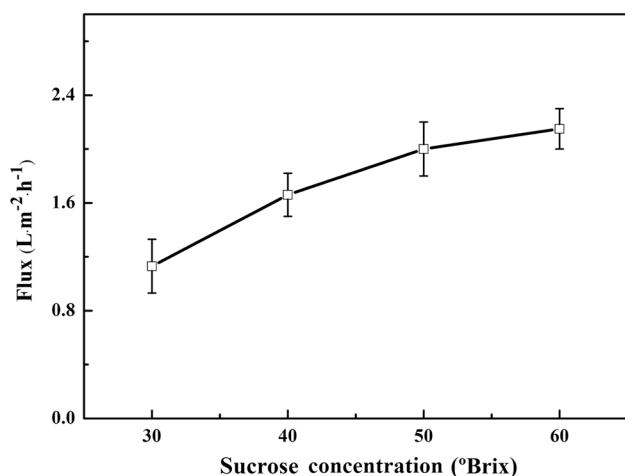


Fig. 4 Effect of sucrose concentration on water flux

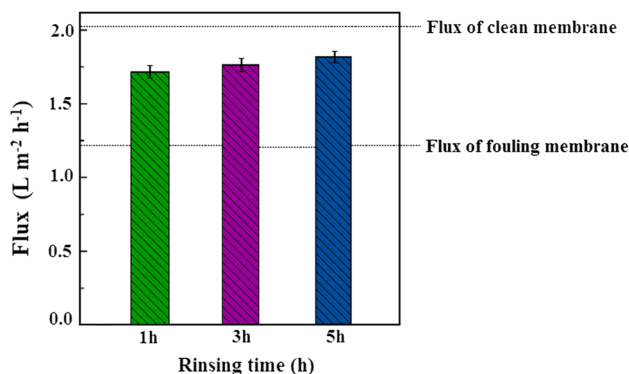


Fig. 5 Comparison of flux after fouling and flux after rinsing

The FO membrane exhibited the best performance with  $2.04 \text{ L m}^{-2} \text{ h}^{-1}$  flux and 98.61% rejection rate.

### Effect of sucrose concentration on water flux

Figure 4 shows the variation of water flux with the sucrose concentration. The flux increases with the increase of sucrose concentration. The reasons are as follows. When the sucrose concentration increased, the osmotic pressure increased, which induced the driving force to become large. Certainly, increasing the sucrose concentration would induce the viscosity to increase, which also made the concentration polarization at the membrane surface in the draw solution to aggravate. However, the increase of water flux caused by the increase of osmotic pressure was a major role and the

concentration polarization caused by the increase of sucrose concentration was only a secondary role. Consequently, using saturated sucrose solution as the draw solution was a good choice in this work.

### Effect of membrane rinsed in reverse

Figure 5 shows flux after rinsing 1, 3, 5 h. We can see that the flux after rinsing is larger than flux after fouling, especially after short-time (1 h) water rinsing. After rinsing for 1 h, the water flux of the FO membrane recovered 87.51%. When the rinsing time is increased to 3 and 5 h, the flux changes are not very obvious. The results show that reverse water rinsing is useful in membrane cleaning.

### Surface morphology and characteristic analysis

Figure 6 shows the scanning electron micrograph of the FO membrane with optimum performance. The membrane had a typical asymmetric structure. The top surface of the membrane is shown in Fig. 6a, which shows a porous structure on this surface. The cross section of the membrane is shown in Fig. 6b. The cross section consisted of three parts, namely surface layer, middle sublayer, and bottom layer. The very compact structure in the upper half of the image was a dense surface layer, which plays the main role in the rejection rate. The middle sublayer, which occupied more than half of the whole thickness, displayed tear-like voids. The bottom layer exhibited a sponge-like porous structure.

For FO membranes, the better the hydrophilicity, the higher the water flux will be. The water contact angle of the FO membrane was  $58^\circ$ , which showed good hydrophilic property. Figure 7 illustrates the ATR-FTIR spectrum of the membrane with optimum performance. The peak at  $3476 \text{ cm}^{-1}$  is in agreement with the O–H stretching vibration of CA. The peak at  $2923 \text{ cm}^{-1}$  is the stretching vibration of C–H. The peak at  $1737 \text{ cm}^{-1}$  is in agreement with the C=O stretching vibration of CA. The peaks at 1431 and  $1367 \text{ cm}^{-1}$  represent the bending vibration of C–H. The three absorption bands at 1034, 1162, and  $1220 \text{ cm}^{-1}$  were attributed to the ether bond of CA. The peak at  $1659 \text{ cm}^{-1}$  (C=C) may be the stretching vibration of rudimental PVP.

### Comparison with published performance of an FO membrane

Several previously published parameters are listed in Table 5 to compare with those of the proposed FO membrane

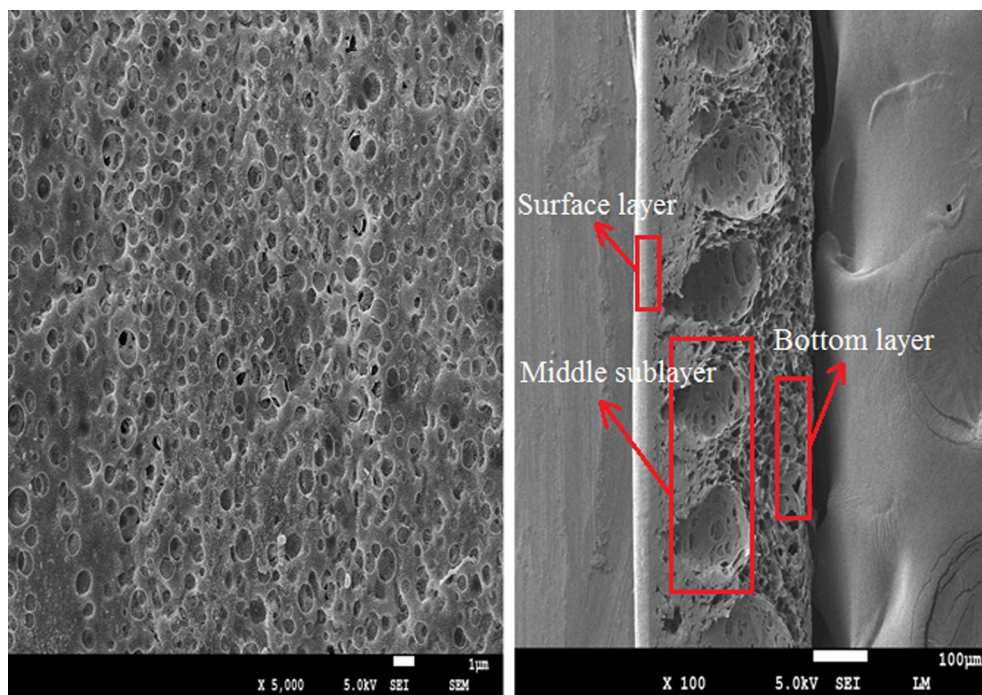


Fig. 6 SEM of the FO membrane with optimum performance: a top surface and b cross section

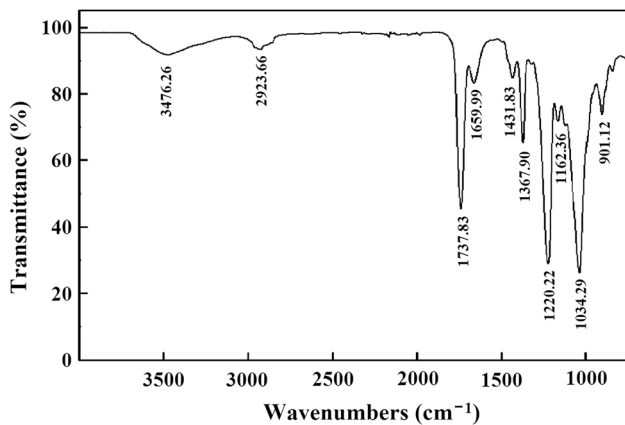


Fig. 7 ATR-FTIR spectrum of the FO membrane with optimum performance

performance for food processing. The flux of the proposed membrane was 1.7 times higher than that obtained by Babu et al. (2006). The present flux was also within the range of that reported by Chanukya and Rastogi (2017), but the proposed membrane showed a higher rejection rate by 1.2-fold. Moreover, the molecular weight of anthocyanin obtained in this study was smaller than those in the two previous studies, but the rejection rate of the proposed membrane still reached 98.61%.

Table 5 Comparison of FO membrane properties for food processing

Membranes name	Feed solution	Main component and molecular weight (g mol <sup>-1</sup> )	Flux (L m <sup>-2</sup> h <sup>-1</sup> )	Rejection (%)
Commercial direct osmosis membrane (Babu et al. 2006)	Pineapple juice	Pectin (~100,000); sucrose (342.3)	1.18	–
Commercial forward osmosis membrane (Chanukya and Rastogi 2017)	Rose extract solution containing anthocyanin	Peonidin-3-glucoside (498.8); delphinidin-3-glucoside (500.8)	11.50–0.50	81.66%
CA forward osmosis membrane	Anthocyanin solution	Cyanidin-3-O-glucoside (449.2)	2.04	98.61%

## Conclusions

In this study, CA FO membranes were fabricated using a phase inversion method. The membrane with optimum performance was applied to concentrate anthocyanin solution. Saturated sucrose solution (about 60° Brix) was fit for using as draw solution. The experimental results showed that the prepared membrane could significantly improve the rejection rate for anthocyanin solution. The permeation properties of the FO membrane were optimized with the following components in the casting solution: 13% CA, 45% 1,4-dioxane, 31% acetone, 2% maleic acid, 3% PVP, and 6% methanol. The water flux was  $2.04 \text{ L m}^{-2} \text{ h}^{-1}$ , and the rejection rate was 98.61%. Reverse water rinsing was used in cleaning membrane that was fouled by anthocyanin solution. When using FO membranes for concentration anthocyanin solution, reverse water rinsing was useful in membrane cleaning. After rinsing 1 h, the water flux of the FO membrane recovered 87.51%.

**Acknowledgements** The authors acknowledge the financial support by Harbin Applied Technology Research and Development Project (2016RAQXJ011).

## References

- Akther N, Sodiq A, Giwa A, Daer S, Arafat HA, Hasan SW (2015) Recent advancements in forward osmosis desalination: a review. *Chem Eng J* 281(1):502–522. <https://doi.org/10.1016/j.cej.2015.05.080>
- Asghar MR, Zhang Y, Wu A, Yan XH, Shen SY, Ke CC, Zhang JL (2018) Preparation of microporous Cellulose/Poly(vinylidene fluoride-hexafluoropropylene) membrane for lithium ion batteries by phase inversion method. *J Power Sources* 379:197–205. <https://doi.org/10.1016/j.jpowsour.2018.01.052>
- Babu J, Murthy ZVP (2017) Treatment of textile dyes containing wastewaters with PES/PVA thin film composite nanofiltration membranes. *Sep Purif Technol* 183:66–72. <https://doi.org/10.1016/j.seppur.2017.04.002>
- Babu BR, Rastogi NK, Raghavarao KSMS (2006) Effect of process parameters on transmembrane flux during direct osmosis. *J Membr Sci* 280:185–194. <https://doi.org/10.1016/j.memsci.2006.01.018>
- Baron G, Altomare A, Regazzoni L, Redaelli V, Grandi S, Riva A, Morazzoni P, Mazzolari A, Carini M, Vistoli G, Aldini G (2017) Pharmacokinetic profile of bilberry anthocyanins in rats and the role of glucose transporters: LC-MS/MS and computational studies. *J Pharm Biomed Anal* 144:112–121. <https://doi.org/10.1016/j.jpba.2017.04.042>
- Boriboon D, Vongssetkul T, Limthongkul P, Kobsiriphat W, Tamawat P (2018) Cellulose ultrafine fibers embedded with titania particles as a high performance and eco-friendly separator for lithium-ion batteries. *Carbohydr Polym* 189:145–151. <https://doi.org/10.1016/j.carbpol.2018.01.077>
- Cath TY, Childress AE, Elimelech M (2006) Forward osmosis: principles, applications, and recent developments. *J Membr Sci* 281(1):70–87. <https://doi.org/10.1016/j.memsci.2006.05.048>
- Chanukya BS, Rastogi NK (2017) Ultrasound assisted forward osmosis concentration of fruit juice and natural colorant. *Ultrason Sonochem* 34:426–435. <https://doi.org/10.1016/j.ultsonch.2016.06.020>
- Chen X, Xu J, Lu J, Shan B, Gao C (2017) Enhanced performance of cellulose triacetate membranes using binary mixed additives for forward osmosis desalination. *Desalination* 405:68–75. <https://doi.org/10.1016/j.desal.2016.12.003>
- Chung TS, Li X, Rui CO, Ge QC, Wang HL, Han G (2012) Emerging forward osmosis (FO) technologies and challenges ahead for clean water and clean energy applications. *Curr Opin Chem Eng* 1(3):246–257. <https://doi.org/10.1016/j.coche.2012.07.004>
- Cui JQ, Liu JQ, He CF, Li J, Wu XF (2017) Composite of polyvinylidene fluoride-cellulose acetate with  $\text{Al}(\text{OH})_3$ , as a separator for high-performance lithium ion battery. *J Membr Sci* 541:661–667. <https://doi.org/10.1016/j.memsci.2017.07.048>
- Etemadi H, Yegani R, Seyfollahi M (2017) The effect of amino functionalized and polyethylene glycol grafted nanodiamond on anti-biofouling properties of cellulose acetate membrane in membrane bioreactor systems. *Sep Purif Technol* 177:350–362. <https://doi.org/10.1016/j.seppur.2017.01.013>
- Gao Y, Fang Z, Liang P, Huang X (2018) Direct concentration of municipal sewage by forward osmosis and membrane fouling behavior. *Bioresour Technol* 247:730–735. <https://doi.org/10.1016/j.biortech.2017.09.145>
- Ge QC, Ling MM, Chung TS (2013) Draw solutions for forward osmosis processes: developments, challenges, and prospects for the future. *J Membr Sci* 442:225–237. <https://doi.org/10.1016/j.memsci.2013.03.046>
- Gray GT, Mccutcheon JR, Elimelech M (2006) Internal concentration polarization in forward osmosis: role of membrane orientation. *Desalination* 197(1–3):1–8. <https://doi.org/10.1016/j.desal.2006.02.003>
- Jafari SM, Ghalenoei MG, Dehnad D (2017) Influence of spray drying on water solubility index, apparent density, and anthocyanin content of pomegranate juice powder. *Powder Technol* 311:59–65. <https://doi.org/10.1016/j.powtec.2017.01.070>
- Jiao B, Cassano A, Drioli E (2004) Recent advances on membrane processes for the concentration of fruit juices: a review. *J Food Eng* 63:303–324. <https://doi.org/10.1016/j.jfoodeng.2003.08.003>
- Law JY, Mohammad AW (2017) Multiple-solute salts as draw solution for osmotic concentration of succinate feed by forward osmosis. *Ind Eng Chem* 51(5):264–270. <https://doi.org/10.1016/j.jiec.2017.03.011>
- Lee S, Boo C, Elimelech M, Elimelech M, Hong S (2010) Comparison of fouling behavior in forward osmosis (FO) and reverse osmosis (RO). *J Membr Sci* 365(1):34–39. <https://doi.org/10.1016/j.memsci.2010.08.036>
- Li JF, Xu ZL, Yang H, Yu LY, Liu M (2009) Effect of  $\text{TiO}_2$  nanoparticles on the surface morphology and performance of microporous PES membrane. *Appl Surf Sci* 255(9):4725–4732. <https://doi.org/10.1016/j.apsusc.2008.07.139>
- Lutchmiah K, Verliefe ARD, Roest K, Rietveld LC, Cornelissen ER (2014) Forward osmosis for application in wastewater treatment: a review. *Water Res* 58(3):179–197. <https://doi.org/10.1016/j.watres.2014.03.045>
- Malek SAA, Seman MNA, Johnson D, Hilal N (2017) Formation and characterization of polyethersulfone membranes using different concentrations of polyvinylpyrrolidone. *Desalination* 288:31–39. <https://doi.org/10.1016/j.desal.2011.12.006>



- Nayak CA, Rastogi NK (2010) Forward osmosis for the concentration of anthocyanin from *Garcinia indica*, Choisy. *Sep Purif Technol* 71(2):144–151. <https://doi.org/10.1016/j.seppur.2009.11.013>
- Petrots KB, Lazarides HN (2001) Osmotic concentration of liquid foods. *J Food Eng* 49:201–206. [https://doi.org/10.1016/S0260-8774\(00\)00222-3](https://doi.org/10.1016/S0260-8774(00)00222-3)
- Phuntsho S, Sahebi S, Majeed T, Lotfi F, Kim JE, Shon HK (2013) Assessing the major factors affecting the performances of forward osmosis and its implications on the desalination process. *Chem Eng J* 231(3):484–496. <https://doi.org/10.1016/j.cej.2013.07.058>
- Qasim M, Mohammed F, Aidan A, Darwish NA (2017) Forward osmosis desalination using ferric sulfate draw solute. *Desalination* 423:12–20. <https://doi.org/10.1016/j.desal.2017.08.019>
- Rabiee H, Vatanpour V, Zarrabi H (2015) Improvement in flux and antifouling properties of PVC ultrafiltration membranes by incorporation of zinc oxide (ZnO) nanoparticles. *Sep Purif Technol* 156:299–310. <https://doi.org/10.1016/j.seppur.2015.10.015>
- Roy D, Rahni M, Pierre P, Yargeau V (2016) Forward osmosis for the concentration and reuse of process saline wastewater. *Chem Eng J* 287:277–284. <https://doi.org/10.1016/j.cej.2015.11.012>
- Sairam M, Sereewatthanawut E, Li K, Bismarck A, Livingston AG (2011) Method for the preparation of cellulose acetate flat sheet composite membranes for forward osmosis—desalination using  $MgSO_4$  draw solution. *Desalination* 273:299–307. <https://doi.org/10.1016/j.desal.2011.01.050>
- Waheed S, Ahmad A, Khan SM, Sabad-e-Gul Jamil T, Islam A, Husain T (2014) Synthesis, characterization, permeation and antibacterial properties of cellulose acetate/polyethylene glycol membranes modified with chitosan. *Desalination* 351:59–69. <https://doi.org/10.1016/j.desal.2014.07.019>
- Xu WX, Chen QZ, Ge QC (2017) Recent advances in forward osmosis (FO) membrane: chemical modifications on membranes for FO processes. *Desalination* 419:101–116. <https://doi.org/10.1016/j.desal.2017.06.007>